http://dx.doi.org/10.5012/bkcs.2014.35.2.349

Articles

Effect of Aluminum Purity on the Pore Formation of Porous Anodic Alumina

Byeol Kim and Jin Seok Lee*

*Department of Chemistry, Sookmyung Women's University, Seoul 140-742, Korea. *E-mail: jinslee@sookmyung.ac.kr*
Received September 23, 2013, Accepted October 14, 2013

Anodic alumina oxide (AAO), a self-ordered hexagonal array, has various applications in nanofabrication such as the fabrication of nanotemplates and other nanostructures. In order to obtain highly ordered porous alumina membranes, a two-step anodization or prepatterning of aluminum are mainly conducted with straight electric field. Electric field is the main driving force for pore growth during anodization. However, impurities in aluminum can disturb the direction of the electric field. To confirm this, we anodized two different aluminum foil samples with high purity (99.999%) and relatively low purity (99.8%), and compared the differences in the surface morphologies of the respective aluminum oxide membranes produced in different electric fields. Branched pores observed in porous alumina surface which was anodized in low-purity aluminum and the size; dimensions of the pores were found to be usually smaller than those obtained from high-purity aluminum. Moreover, anodization at high voltage proceeds to a significant level of conversion because of the high speed of the directional electric field. Consequently, anodic alumina membrane of a specific morphology, *i.e.*, meshed pore, was produced.

Key Words : Porous anodic alumina, Impurities, Electric field, Branched pore, Meshed pore

Introduction

Recently, porous anodic aluminum oxide (AAO), a highly ordered nano-pore array, has attracted considerable attention as a nanotemplate for the synthesis of various nanostructures,[1] such as nanowires,[2-4] nanotubes,[5] nanodots,[6,7] semiconductors,[4,8] and superconductors.[9] These applications involve electrochemical deposition,[2,3] atomic layer deposition,[6,7] and chemical vapor deposition.[10] Porous alumina membrane formed by the anodization of aluminum consists of a close-packed array of hexagonal cells, each containing a cylindrical central pore. These pores are extended down to the barrier layer, which is a continuous, non-porous dielectric oxide layer between the pore bottom and the aluminum.[11] Moreover, pore diameter (D_p) and interpore distance (D_{int}) can be adjusted by anodization conditions such as the type of the electrolyte,[12-16] anodizing potential,[13,16] current density,[17] and temperature,[18] The most important factors affecting D_{int} are the chemical composition of the electrolyte and anodizing potential. Sulfuric acid,[12,13] oxalic acid,[12,18] and phosphoric acid[12,14] are most commonly used electrolytes, each of which is used with a specific applied potential.[12-18] In general, anodic alumina membranes can be obtained within three well-known growth regimes: sulfuric acid at 25 V for D_{int} of 63 nm,[12,13,19] oxalic acid at 40 V for D_{int} of 100 nm,[12,18,20] and phosphoric acid at 195 V for D_{int} of 500 nm.[12,14] Moreover, D_p can be modified with pore widening process after anodization. The configuration of pores affected porosity and pore density, which are characteristic of anodic alumina membranes.

However, these characteristic factors were distinguished at anodization using a high purity aluminum foil (99.999%). Most reports on the anodizing of aluminum use high-purity aluminum for improving the quality of porous alumina membranes.[1-19] However, few studies have been conducted on the anodization of low-purity aluminum.[21-29] Fabrication of anodic alumina membranes from low-purity aluminum foil is not trivial and often requires specific conditions, different from those typically applied to the anodization of high-purity aluminum.[29]

Herein, we use two different aluminum foils which are high purity (99.999%) and relatively low purity (99.8%) to fabricate a porous alumina membrane. The anodization was preceded by two-step process[20] under same conditions in oxalic acid with 40 V. In phosphoric acid condition, aluminum was anodized at 190 V for the distinct divisions of two types of purity. We think that impurities of aluminum can disturb the direction of the electric field, the main driving force for the pore formation during anodization. We compare surface morphologies of aluminum oxide to demonstrate the effect of changed electric field due to impurity of aluminum, and describe the effect of aluminum purity on the formation of anodic alumina pores during anodization. Furthermore, we provide the possibility of fabricating a novel nanostructure using low-purity aluminum.

Experimental

A high purity aluminum foil (99.999%, Good fellow) and relatively low purity aluminum foil (99.8%, Sigma Aldrich)

were cut into specimens (2 × 3 cm) with the working area of 4 cm^2. Aluminum foil was degreased in acetone and washed in deionized water. Then, the sheet was annealed under argon atmosphere at 500 °C in order to enhance the grain size in the metal and to obtain homogenous conditions for pore growth.[30] After this, the foil was electropolished in a mixture of perchloric acid ($HClO_4$) and ethyl alcohol (C_2H_5OH) (volume ratio 1:4) at constant potential of 10 V for 3 min to diminish the roughness of the aluminum surface.[31] The sample was anodized in a 0.3 M oxalic acid solution at 40 V for 1 h, under constant temperature at 10 °C. The other sample was anodized under 0.1 M phosphoric acid solution at 190 V and 1 °C. After anodization, random and disordered pores were obtained. Formed anodic aluminum oxide layer was chemically removed by a mixture of 6 wt % H_3PO_4 and 1.8 wt % CrO_3 at 50 °C for 30 min. The second anodization was carried out under the same condition as were used during the first anodization step for 30 min. After this, the pores were opened in a same mixture of etching solution at 30 °C for 10 min. During experimental, in order to keep the constant electrolyte temperature, a double walled bath with a refrigerated circuiting system is used. The morphology of porous alumina film was evaluated by a field emission scanning electron microscope (FE-SEM).

Results and Discussion

We proposed that electric field is the main driving force for the pore growth during anodization and impurities in the aluminum disturb the direction of electric field. Therefore, we carefully compared the morphologies of anodized alumina membranes and the changes in the electric field as a function of aluminum purity.

To fabricate a porous alumina membrane, we used two different aluminum foil samples with high purity (99.999%, Al_{high}) and relatively low purity (99.8%, Al_{low}), respectively. The anodization process was preceded by a two-step process[20] in oxalic acid at 40 V and phosphoric acid at 190 V for high- and low-purity aluminum samples, respectively.

Figure 1 shows the scanning electron microscopy (SEM) images of Al_{low} (Figures 1(a) and 1(b)) and Al_{high} (Figures 1(c) and 1(d)) anodized by a two-step process in 0.3 M oxalic acid solution at 10 °C. The applied potential was 40 V and the anodization duration was 1 h. The surface of anodized Al_{low} exhibits a disordered array of nanopores with different pore sizes (Figure 1(a)). Longer first-anodizing duration results in better ordering of the pores array in the two-step anodizing process.[32] Hence, we expected to obtain higher regularity ratio, circularity, and lower concentration of defects in the resulting anodic alumina. However, we observed that the surface of anodized Al_{low} unfavorably influences the regularity ratio, circularity, and defects, which had been also observed by others.[29] Interestingly, the majority of nanopores of anodized Al_{low} were found to consist of branched pores that had additional pores located near the main pore, which we attribute to defects formed during pore formation. Figure 1(b) shows a low-magnified SEM image of anodized Al_{low}, with the branched pores shown in red. Most pores appear highly disordered and branched. Because using Al_{low} for anodization increases the defects, we consider Al_{low} unsuitable for fabricating a highly ordered pore array.

Therefore, we conducted the two-step anodization process of Al_{high} under the conditions used for Al_{low} in order to investigate the effect of aluminum purity on the geometry of anodized pores. As shown in Figure 1(c), the surface of anodized Al_{high} exhibits fewer pore defects and better circularity of pores than the surface of anodized Al_{low}. The majority of pores which are anodized at Al_{high} is straight and single (not double or triple). Accordingly, the degree of branched pore for Al_{high} is less than that of Al_{low} (Figures 1(b) and 1(d)). Based on these observations, we confirmed that the purity of aluminum foil strongly affects the pore geometry.

The effect of aluminum purity on the geometry of anodized pores can be more accurately observed by investigating the size of D_p and D_{int}. Figure 2 shows D_p and D_{int} for pores

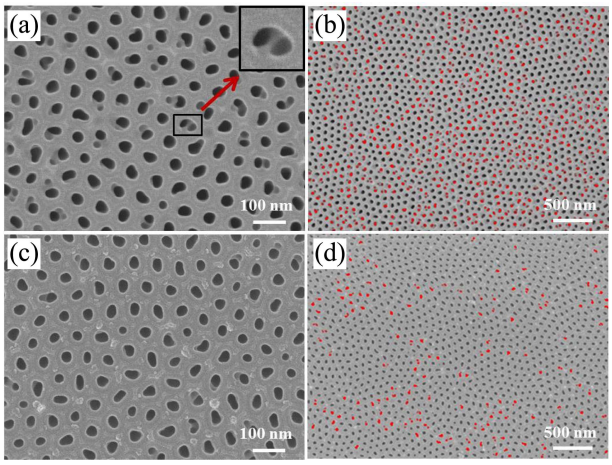

Figure 1. SEM images of Al_{low} (a, b) and Al_{high} (c, d) anodized in a two-step process in 0.3 M oxalic acid solution at 10 °C and 40 V for 1 h. Branched pores are represented as red in (b) and (d).

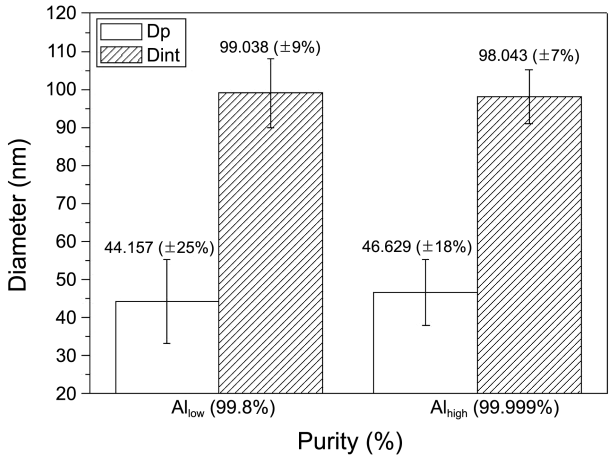

Figure 2. The histogram of average size of pore diameter (D_p) and interpore distance (D_{int}) in anodized Al_{low} and Al_{high}, respectively. Standard deviations are shown in parentheses.

formed by anodization in 0.3 M oxalic acid solution at 10 °C and 40 V for 1 h. It was well known that D_{int} of anodic alumina under ordinary anodizing conditions linearly increases on increasing the applied anodizing voltage. The voltage dependence of D_{int} is given as

$$D_{int} = \zeta U$$

where ζ is approximate at 2.5 nm/V and U is the applied potential.[33] From this relationship, D_{int} for anodization at 40 V is calculated to be 100 nm, similar aspect for both Al_{high} and Al_{low}. However, nanopores in anodized Al_{low} have larger standard deviation in D_{int} compared to those in anodized Al_{high}. Similar tendency is appeared in D_p. The size of D_p is influenced by the pore-widening duration after anodization.[34] Therefore, we used a fixed pore-widening duration of 10 min in a mixture of 6 wt % phosphoric acid and 1.8 wt % chromium(VI) oxide at 30 °C in order to investigate the effect of aluminum purity on D_p. As shown in Figure 2, the D_p of anodized Al_{low} is small relative to anodized Al_{high}. Aluminum ions originating from the foil dissolve and form aluminum oxide after oxidation during anodization.[28] It is expected that impurities in Al_{low} limit the oxidation reaction, albeit to a small degree. During the anodization of Al_{low}, the formation of aluminum oxide is prevented by the impurities and nonuniformly progresses on the aluminum foil surface. Therefore, nanopores of anodized Al_{low} have smaller D_p and large standard deviation compared to those of anodized Al_{high}.

To confirm an effect of aluminum purity on anodization, we conducted the two-step anodization process with Al_{low} and Al_{high} in 0.1 M phosphoric acid solution at 1 °C.[14] The applied potential was 190 V and the anodization duration was 3 h. Figure 3 shows the SEM images of anodized Al_{low} (Figures 3(a) and 3(b)) and anodized Al_{high} (Figures 3(c) and 3(d)). Interestingly, the surface of anodized Al_{low} show unique, mesh-like pore geometry. The phenomenon of branched pores is more pronounced in phosphoric acid compared to

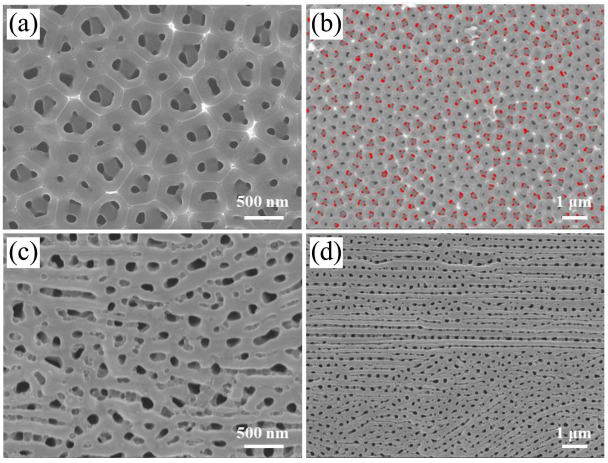

Figure 3. SEM images of Al_{low} (a, b) and Al_{high} (c, d) anodized in 0.1 M phosphoric acid solution at 1 °C. Applied potential and anodization time were 190 V and 3 h, respectively. Meshed and branched pores are represented to red color in (b).

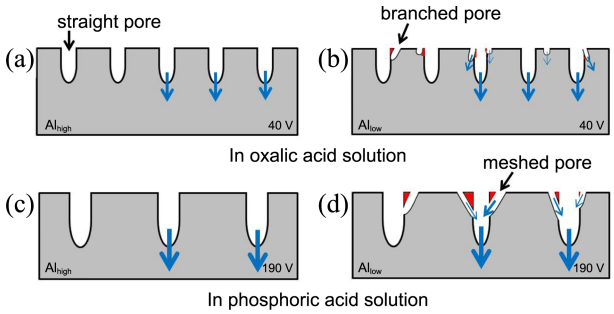

Figure 4. Schematic illustration of the pore formation on Al_{high} (a, c) and Al_{low} (b, d) in oxalic acid solution at 40 V (a, b) and in phosphoric acid solution at 190 V (c, d).

anodization in oxalic acid at 40 V. Figure 3(b) shows the degree of defects (in red), including meshed and branched pores. The majority of nanopores exhibit double or triple pores on the surface of anodized Al_{low}. To compare pore geometry, we also conducted the anodization of Al_{high} under the same conditions as those of anodized Al_{low}. The surface of anodized Al_{high} exhibited fewer pore defects and straight nanopores compared to that of anodized Al_{low} (Figure 3(c)). The above difference in the anodized surface of Al_{high} and Al_{low} further supports that the effect of aluminum purity on the geometry of pores could be enhanced by increasing the applied potential.

We attribute the above differences in pore geometry to the process of pore formation during the anodization of Al_{high} and Al_{low} with different acidic solutions and applied potentials (Figure 4). The pore nucleation theory, which is based on the field-enhanced oxide dissolution, explained that pores grow perpendicular to the aluminum substrate with equilibrium of field-enhanced oxide dissolution at the oxide/electrolyte interface and oxide growth at the metal/oxide interface.[30] According to recent studies, anion species migrate into the oxide film formed on the surface of the aluminum substrate during anodization, leading to considerable accumulation of impurities in the barrier layer.[35] Moreover, it has been reported that if some impurities exist at the metal/oxide interface, where the oxide grows primarily, the growth of aluminum oxide can be blocked.[35,36] The local accumulation of alloying elements in a given region of the metal/oxide interface changes the local rates of oxidation. This difference of oxidation rate, which is originated from impurities, can result in nonuniformity thickness of the aluminum oxide layer. Thus, irregular directions of electric field have also been shown to be induced by impurities.[28,29] Based on the fact that the direction of electric field applied to aluminum substrate affects the geometry of pores,[37] pores with branched and meshed geometries found on the surface of anodized Al_{low} could result from the irregular directions of the electric field (Figures 4(b) and 4(d), respectively). Moreover, irregular formation of pores on the surface of Al_{low} could accelerate on increasing the applied potential as the strength of the electric field is increased. This observation explains the extremely disordered pore array (meshed pores; Figure 4(d)) formed on the surface of Al_{low} in phosphoric acid at 190 V.

Conclusion

We investigated the effect of aluminum purity (Al_{high}, 99.999% and Al_{low}, 99.8%) on the pore formation of porous anodic alumina membranes. The specific morphology parameters D_p and D_{int} were estimated from the SEM images. The D_{int} values of these two porous alumina surfaces were found to be similar because D_{int} is directly proportional to the applied anodizing potential. The D_p of alumina membranes formed by two-step anodizing of Al_{low} was smaller than that of Al_{high} in oxalic acid condition, thus confirming that aluminum impurities influenced aluminum oxidation. Moreover, more branched pore defects were produced during the anodization of Al_{low} than that of Al_{high}. Likewise, the purity of the aluminum foil samples influenced the morphologies of alumina films after anodization, resulting in the formation of branched pores in the membrane. Furthermore, during the anodization of Al_{low} at 190 V, electric fields dramatically changed their direction, leading to a characteristic morphology–meshed pores; in contrast, standard pores exhibit straight channels in the oxide film. Anodic alumina anodized in phosphoric acid has large superficial dimension, although the mesh pore array is not highly ordered. This array is can be useful for the fabrication of specific substrates. The high surface area of meshed pores can be advantageous in many applications such as gas adsorption.

Acknowledgments. This study was supported by the SRC Research Center for Women's Diseases of Sookmyung Women's University (2011).

References

1. Sulka, G. D.; Zaraska, L.; Stępniowski, W. J. In *Encyclopedia of Nanoscience and Nanotechnology*, 2nd ed.; Nalwa, H. S., Ed.; American Scientific Publishers: Valencia, 2011; Vol. 11, pp 261-349.
2. Sulka, G. D.; Brzózka, A.; Zaraska, L.; Jaskuła, M. *Electrochim. Acta* **2010**, *55*, 4368.
3. Ohgai, T.; Hoffer, X.; Fabian, A.; Gravier, L.; Ansermet, J.-P. *J. Mater. Chem.* **2003**, *13*, 2530.
4. Mondal, S. P.; Das, K.; Dhar, A.; Ray, S. K. *Nanotechnology* **2007**, *18*, 095606.
5. Lee, W.; Scholz, R.; Nielsch, K.; Gösele, U. *Angew. Chem., Int. Ed. Engl.* **2005**, *44*, 6050.
6. Johansson, A.; Törndahl, T.; Ottosson, L. M.; Boman, M.; Carlsson, J.-O. *Mater. Sci. Eng., C, Biomim. Mater. Sens. Syst.* **2003**, *23*, 823.
7. Elam, J. W.; Zinovev, A.; Han, C. Y.; Wang, H. H.; Welp, U.; Hryn, J. N.; Pellin, M. J. *Thin Solid Films* **2006**, *515*, 1664.
8. Gaponenko, V.; Molchan, I. S.; Tsyrkunov, D. A.; Maliarevich, G. K.; Aegerter, M.; Puetz, J.; Al-Dahoudi, N.; Misiewicz, J.; Kudrawiec, R.; Lambertini, V.; Li Pira, N.; Repetto, P. *Microelectron. Eng.* **2005**, *81*, 255.
9. Jian, X.; Xiaohe, L.; Yadong, L. *Mater. Chem. Phys.* **2004**, *86*, 409.
10. Chen, P.; Chua, S. J.; Wang, Y. D.; Sander, M. D.; Fonsta, C. G. *Appl. Phys. Lett.* **2005**, *87*, 143111.
11. Lei, Y. *et al*. *Progress in Materials Science* **2007**, *52*, 465-539.
12. Li, A. P.; Müller, F.; Birner, A.; Nielsch, K.; Gösele, U. *J. Appl. Phys.* **1998**, *84*, 6023.
13. Zhang, F.; Liu, X.; Pan, C.; Zhul, J. *Nanotechnology* **2007**, *18*, 345302.
14. Masuda, H.; Yada, K.; Osaka, A. *Jpn. J. Appl. Phys.* **1998**, *37*, 1340.
15. Chung, C.-K.; Liu, T. Y.; Chang, W. T. *Microsyst Technol.* **2010**, *16*, 1451-1456.
16. Friedman, A. L.; Brittain, D.; Menon, L. *J. Chem. Phys.* **2007**, *127*, 154717.
17. Zhoua, F.; Baron-Wiecheća, A.; Garcia-Vergarab, S. J.; Curionia, M.; Habazakic, H.; Skeldona, P.; Thompsona, G. E. *Electrochimica Acta* **2012**, *59*, 186-195.
18. Kashi, M. A.; Ramazani, A. *J. Phys. D: Appl. Phys.* **2005**, *38*, 2396-2399.
19. Masuda, H.; Hasegwa, F.; Ono, S. *J. Electrochem. Soc.* **1997**, *144*, L127.
20. Masuda, H.; Fukuda, K. *Science* **1995**, *268*, 1466.
21. Montero-Moreno, J. M.; Sarret, M.; Müller, C. *J. Electrochem. Soc.* **2007**, *154*, C169.
22. Aerts, T.; Dimogerontakis, Th.; De Graeve, I.; Fransaer, J.; Tercyn, H. *Surf. Coat. Technol.* **2007**, *201*, 7310.
23. Yu, Ch-U.; Hu, Ch-Ch.; Bai, A.; Yang, Y.-F. *Surf. Coat. Technol.* **2007**, *201*, 7259.
24. Bai, A.; Hu, Ch-Ch.; Yang, Y.-F.; Lin, Ch-Ch. *Electrochim. Acta* **2008**, *53*, 2258.
25. Shih, T.-S.; Wei, P.-S.; Huang, Y.-S. *Surf. Coat. Technol.* **2008**, *202*, 3298.
26. Montero-Moreno, J. M.; Belenguer, M.; Sarret, M.; Müller, C. M. *Electrochim. Acta* **2009**, *54*, 2529.
27. Fernández-Romero, L.; Montero-Moreno, J. M.; Pellicer, E.; Peiró, F.; Cornet, A.; Morante, J. R.; Sarret, M.; Müller, C. *Mater. Chem. Phys.* **2008**, *111*, 542.
28. Chen, C. C.; Chen, J. H.; Chao, C. G. *Jpn. J. Appl. Phys.* **2005**, *44*(3), 1529.
29. Zaraska, L. *et al*. *Electrochimica Acta* **2010**, *55*, 4377-4386.
30. Jessensky, O.; Müller, F.; Gösele, U. *Appl. Phys. Lett.* **1998**, *72*, 1173.
31. Rauf, A.; Mehmood, M.; Rasheed, M. A.; Aslam, M. *J. Solid State Electrochem.* **2009**, *13*, 321-332.
32. Stępniowski, W. J.; Zasada, D.; Bojar, Z. *Surface & Coatings Technology* **2011**, *206*, 1416-1422.
33. Lee, W.; Ji, R.; Gösele, U.; Nielsch, K. *Nature Mater.* **2006**, *5*, 741-747.
34. Lee, W.; Han, H.; Park, S.-J.; Jang, J. S.; Ryu, H.; Kim, K. J.; Baik, S. *ACS Appl. Mater. Interfaces* **2013**, *5*, 3441-3448.
35. Fratila-Apachitei, L. E.; Tichelaar, F. D.; Thompson, G. E.; Terryn, H.; Skeldon, P.; Duszczyk, J.; Katgerman, L. *Electrochim. Acta* **2004**, *49*, 3169.
36. Mukhopadhyay, K.; Sharma, A. K. *Surf. Coat. Technol.* **1997**, *92*, 212.
37. Lu, J. G.; Li, D.; Zhao, L.; Jiang, C. *Nano Lett.* **2010**, *10*, 2766-2771.